*J. Anat.* (1999) **195**, pp. 121–130, with 3 figures Printed in the United Kingdom 

# Electron-immunocytochemical studies of perivascular nerves of mesenteric and renal arteries of golden hamsters during and after arousal from hibernation

**PORNCHARN SAITONGDEE[1]*, PAMELA MILNER[2], ANDRZEJ LOESCH[1], GILLIAN KNIGHT[1] AND GEOFFREY BURNSTOCK[2]**

[1] *Department of Anatomy and Developmental Biology, University College London, and* [2] *Autonomic Neuroscience Institute, Royal Free and University College Medical School, London, UK*

(*Accepted 13 April 1999*)

ABSTRACT

Electron immunocytochemistry was used to examine perivascular nerves of hamster mesenteric and renal arteries during hibernation and 2 h after arousal from hibernation. Vessels from cold-exposed but nonhibernating, and normothermic control hamsters were also examined. During hibernation the percentage of axon profiles in mesenteric and renal arteries that were immunopositive for markers of sympathetic nerves, tyrosine hydroxylase (TH) and neuropeptide Y (NPY), were increased 2–3 fold compared with normothermic and cold control animals. This increase was reduced markedly only 2 h after arousal from hibernation. The small percentage of nitric oxide synthase-1-positive axon profiles found in mesenteric (but not renal) arteries was also increased during hibernation and returned towards control values after arousal. In contrast, the percentage of perivascular axons immunostaining for vasoactive intestinal polypeptide (VIP), a marker for parasympathetic nerves, was reduced in mesenteric arteries during hibernation. There was no labelling of perivascular nerves for substance P in either mesenteric or renal arteries. It is suggested that the increase in percentage of TH- and NPY-immunostained perivascular nerves may account for the increased vasoconstriction associated with high vascular resistance that is known to occur during hibernation. The reduction in the percentage of axons positive for VIP in hibernating animals would contribute to this mechanism since this neuropeptide is a vasodilator.

*Key words*: Tyrosine hydroxylase; neuropeptide Y; vasoactive intestinal peptide; substance P; nitric oxide synthase.

## INTRODUCTION

In mammals, hibernation represents an effective strategy for surviving periods of harsh ecological conditions, a scarcity of food and adverse low temperature weather conditions. The physiological change from the normothermic condition to the state of hibernation is characterised by a decrease in metabolic rate and body temperature to below 10 °C, a reduced heart rate to below 10 beats/min, reduced respiratory rate of less than 3 breaths/min, a decrease in systemic blood pressure to about 50 mmHg, but an increase in peripheral vascular resistance (Lyman, 1965; Nedergaard & Cannon, 1990; Nürnberger, 1995). Food intake and gut function are suspended and renal function is reduced. Arousal is rapid and starts with an increase in heart rate, respiration and oxygen consumption, followed by a rise in body temperature and regulation of vasodilatation which leads to an increase in blood pressure and blood flow (Chatfield & Lyman, 1950; Lyman, 1965; Lyman & O'Brien, 1988).

Vasodilatation and vasoconstriction respectively, are fundamental physiological adjustments to increased and decreased metabolic demands by tissues. The changes of peripheral vascular resistance to allow

Correspondence to Professor G. Burnstock, Autonomic Neuroscience Institute, Royal Free and University College Medical School, Rowland Hill Street, London NW3 2PF, UK. Tel.: +44171 830 2948; fax: +44171 830 2949.
* Permanent address: Department of Anatomy, Faculty of Science, Mahidol University, Bangkok, Thailand.

blood flow are mediated by dual local control, by endothelial cells and perivascular nerves (Burnstock & Ralevic, 1994). Sympathetic nerves exert vasoconstrictor tone in most blood vessels, utilising noradrenaline (NA), adenosine 5′-triphosphate (ATP) and neuropeptide Y (NPY). Antibodies to tyrosine hydroxylase (TH), a rate-limiting enzyme involved in the synthesis of catecholamines, and NPY, can be used to examine changes in sympathetic nerves, whereas antibodies to vasoactive intestinal polypeptide (VIP), a potent vasodilator, can be used as an immunomarker for parasympathetic nerves. Nitric oxide (NO) which acts as a potent vasodilator in mesenteric and renal arteries in various mammalian species (Yoshida et al. 1993; Okamura et al. 1995; Vials et al. 1997) is probably released from perivascular sensory-motor nerves during axon reflex activity (Holzer et al. 1995) or may be associated with parasympathetic nerves (Nozaki et al. 1993). In some species nitric oxide synthase (NOS) has also been localised in neurons of sympathetic ganglia (Sheng et al. 1993; Hisa et al. 1995). Substance P (SP) and calcitonin gene-related peptide (CGRP) are localised in sensory-motor nerves, i.e. primary afferent nerve fibres which also have an efferent function (Maggi & Meli, 1988).

There is pharmacological evidence for an increase in sympathetic neurotransmission in mesenteric arteries and renal arteries in the hamster during hibernation, whilst endothelium dependent responses are unchanged (Ralevic et al. 1997; Karoon et al. 1998). A reduction of both vasodilator (NO) and vasoconstrictor (endothelin) elements in mesenteric and renal artery endothelium during hibernation (Saitongdee et al. 1999) as peripheral vascular resistance increases, suggests that neural control may be the predominant mechanism involved in this situation.

The aim of the present study was to examine, at the ultrastructural level, the distribution of immunoreactivity to TH and NPY (markers for sympathetic nerves); VIP (a marker for parasympathetic nerves); NOS-I (the enzyme involved in NO synthesis) and SP (a marker for sensory-motor nerves) in the mesenteric and renal vasculature of hamsters during and after arousal from hibernation.

## MATERIALS AND METHODS

### *Induction of hibernation and arousal*

Adult male golden hamsters (*Mesocricetus auratus*) were used in this study as follows: (I) normothermic control animals maintained in normal animal housing conditions (n = 3), (II) cold-exposed controls maintained under conditions conducive to hibernation (see below) that failed to hibernate (n = 3), (III) hibernating hamsters maintained under conditions conducive to hibernation that underwent hibernation (n = 2), and (IV) hibernating hamsters that were examined 2 h after being brought to room temperature surroundings to arouse from hibernation (n = 2).

Normothermic control animals (group I) were housed at room temperature (20 °C) and exposed to 8 h and 16 h of light and dark periods, respectively. Hibernation was induced by creating 'pseudo' winter conditions. Animals maintained under conditions conducive to hibernation (groups II, III and IV) were initially housed in a refrigerated incubator (Leec Ltd, Nottingham, UK) with the light and dark periods set at 8 h and 16 h, respectively. The period of light was then reduced by 30 min/d, together with a gradual temperature reduction to reach the final conditions of 2 h light per day and 9 °C (this acclimatisation procedure took 7–10 d). The animals were next transferred to individual cages in a cold room which was set at 5 °C with 2 h of light per day and with food and water ad libitum. Sufficient nesting material was also supplied. Inspection of the animals outside the designated light period was only performed under a 10 W red photographic light. To check whether the animals were hibernating, sawdust was sprinkled on their backs (which would wake a sleeping but not a hibernating hamster). After a period of approximately 10 wk, hamsters began to hibernate. Animals were allowed to hibernate for 8 wk, which included natural periodic arousal (for approximately 24 h every 3–5 d). Hamsters were killed only after a deep continuous hibernation bout of 3 d (group III). Hamsters allowed to arouse for 2 h were taken from this hibernating group (group IV). The cheek pouch and rectal temperatures of the hamsters were measured.

### *Perfusion and processing of vessels*

For pre-embedding electron immunocytochemistry, the animals were anaesthetised with sodium pentobarbitone (Sagatal, 60 mg/kg i.p.) and perfused through the heart (left ventricle) with fixative containing 4% paraformaldehyde and 0.1% glutaraldehyde in 0.1 M phosphate buffer pH 7.4 (at room temperature) for 15 min. After perfusion, superior mesenteric and renal arteries were dissected, immersion-fixed for 5 h at 4 °C, then washed with phosphate buffer and thereafter cryoprotected overnight at 4 °C in 7% sucrose in phosphate-buffer (pH 7.4). The following day the arteries were oriented and embedded

in Tissue-Tek (Miles Inc., Elkhart, IN, USA), frozen by immersion in precooled isopentane in liquid nitrogen, and stored in liquid nitrogen until sectioning. Transverse cryosections (50 μm) were cut, after washing several times in phosphate buffer. The specimens were subsequently processed for pre-embedding electron immunocytochemistry of TH, NPY, NOS-I, VIP, and SP using the peroxidase-antiperoxidase (PAP) technique.

### *Immunocytochemistry*

The method used for immunocytochemistry has previously been used to study hamster vascular endothelium (Saitongdee et al. 1999). In the present study, for valid comparisons, samples of superior mesenteric artery and renal artery from all groups were processed for immunolabelling for a particular antigen at the same time. Specimens were exposed for 30 min to 0.3 % hydrogen peroxide in 30 % methanol (to block endogenous peroxidase), washed for 1 h in 0.1 M Tris buffer at pH 7.4 (Tris-1), and then incubated for 1 h in normal goat serum (Nordic Immunology, Tilburg, The Netherlands) diluted 1:30 in Tris containing 0.1 % sodium azide (Tris-2). After washing in Tris-1, the specimens were incubated for 48 h at 4 °C in primary antisera diluted in Tris-2 as follows: TH, 1:500; NPY, NOS-I, VIP and SP, 1:1000. After washing in Tris-1, the specimens were exposed for 1.5 h to goat-antirabbit immunoglobulin G serum (Biogenesis, Bournemouth, UK) diluted 1:50, then rinsed in Tris-1. The specimens were incubated for 2.5 h with a rabbit PAP complex (Dako, Glostrup, Denmark) diluted 1:75, then rinsed in Tris-1. After exposure to 3′3′-diaminobenzidine (Sigma, Poole, UK) and hydrogen peroxide, the specimens were postfixed in 1 % osmium tetroxide, dehydrated in a graded ethanol series and embedded in Araldite. Ultrathin sections were stained with uranyl acetate and lead citrate and subsequently examined with a JEM-1010 electron microscope.

### *Immunocytochemical controls*

The rabbit antisera used in this study were polyclonal and have been characterised by the manufacturers (antisera to TH, Eugene Tech International; NPY, UC Bioproducts, Belgium; NOS-I, N31030, Transduction Laboratories, Lexington, USA; VIP and SP, CRB, Cambridge, UK). In the present study, the specificity of the immunostaining was tested by omission of primary antisera from the incubation medium and/or replacing the primary antisera with normal rabbit serum (Nordic Immunology, Tilburg, The Netherlands) at a dilution of 1:1000, and by preabsorption of the primary antisera for 24 h at 4 °C with a 1 μM solution of the appropriate antigen. NOS-I was preabsorbed with rat pituitary lysate (Transduction Laboratories, Lexington, USA). No immunoprecipitate was observed in these control preparations.

### *Measurement of percentage of immunopositive cells*

In order to establish the percentage of axon profiles positive and negative for a given antigen, axons were counted in ultrathin sections taken from different levels of specimens separated from each other by a distance of $\sim 50$ μm. Axon profiles were counted at a magnification of $\times 6000$–$10000$ by examination with an electron microscope (JEM 1010). Results were expressed as mean $\pm$ standard error of the mean (S.E.M.) of the percentage of immunopositive axons per section of artery from normothermic, cold-exposed, hibernating and aroused animals; at least 12 sections were examined per animal group, with a minimum of 830 axon profiles per group. Statistical analysis of these data, based on the number of sections examined, was carried out using Tukey's test for multiple comparisons, taking $P < 0.05$ as significant.

## RESULTS

### *Animals*

There was a difference in cheek pouch and rectal temperatures among the 4 groups of hamsters. The cheek pouch temperature of the hibernating hamsters was 8 °C compared with 35 °C for both control groups and 33 °C for the arousal group. The rectal temperature of the hibernators was 9 °C compared with 33 °C for both control groups and 32 °C for the arousal group. These temperatures were within the range of previously reported values from a larger number of animals (Saitongdee et al. 1999).

### *Ultrastructure of perivascular nerves*

Perivascular nerves were observed both in mesenteric and renal arteries. The nerve profiles were covered incompletely by Schwann cells and were rich in both varicosities and intervaricosities. Varicosities con-

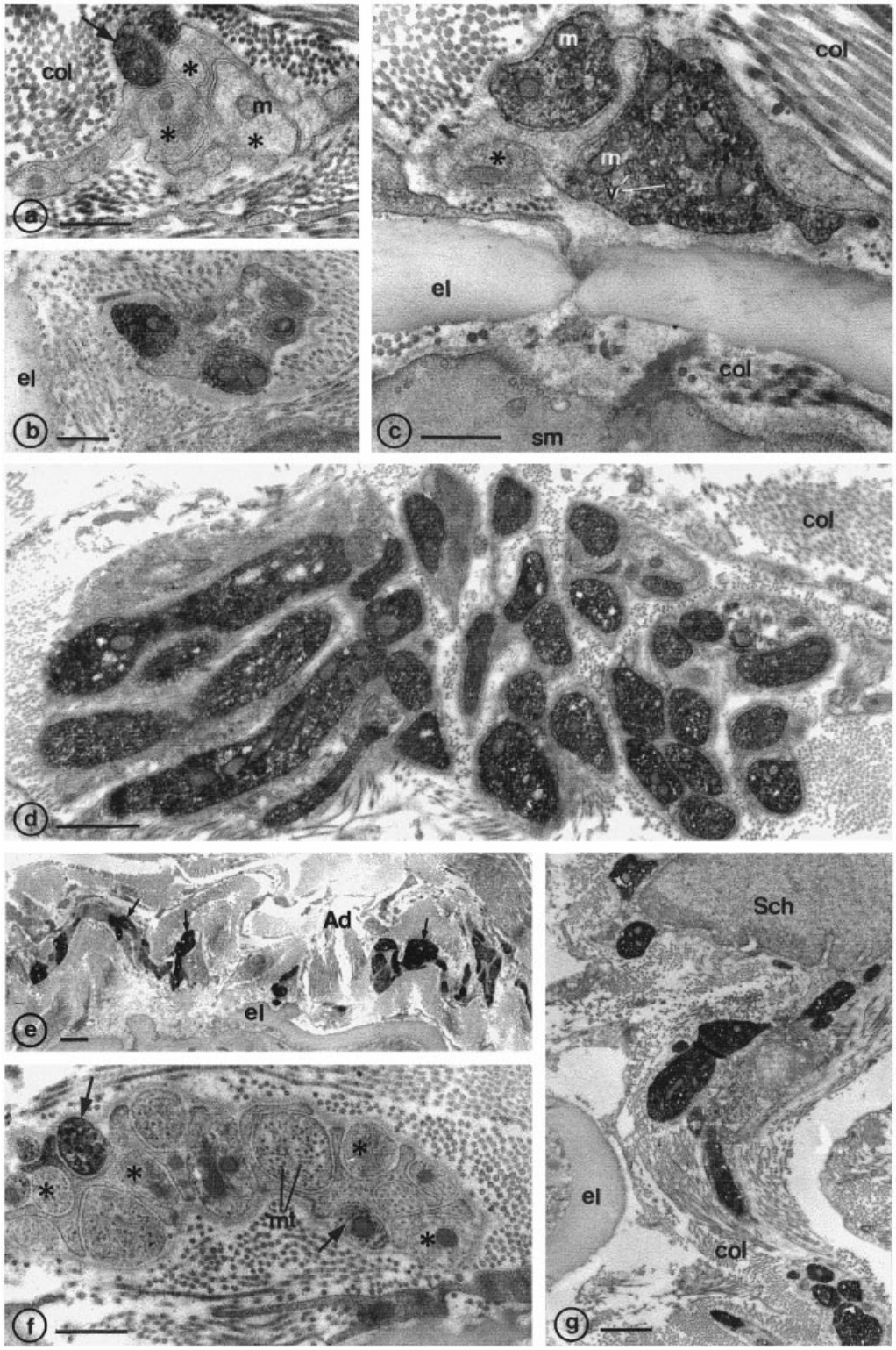


Fig. 1. Mesenteric artery (*a*, *c*, *d*, *f*) and renal artery (*b*, *e*, *g*) labelled for TH in normothermic control (*a*, *b*), cold control (*c*), hibernating (*d*, *e*) and aroused (*f*, *g*) hamsters. (*a*) Two TH-positive (arrow) and several TH-negative (asterisks) axon profiles are seen in a nerve bundle; m, mitochondrion; col, collagen fibres. (*b*) Three TH- positive axons in a nerve bundle are close to the external elastic lamina (el). (*c*) Higher magnification of TH-positive varicosities showing immunoreactive particles in axoplasm, and associated with the membranes of mitochondria and vesicles (v). An unlabelled axon can also be seen (asterisk). sm, Smooth muscle. (*d*) Most of the axon profiles in several nerve bundles showing heavy positive labelling for TH. Both longitudinally and transversely oriented axon profiles are present. (*e*) Low magnification micrograph showing a large number of TH-positive axons (arrows) distributed closely to external elastic lamina at adventitial medial border. Ad, Adventitia. (*f*) At least 2 TH-positive axons (arrows) among several TH-negative axon profiles (asterisks) are seen in a nerve bundle. mt, Microtubules. (*g*) A nerve bundle showing the TH-positive axon profiles associated with Schwann cell (Sch). Bars: *a*, *b*, *c*, *f*, 500 nm; *d*, *e*, *g*, 1 μm.

tained small or large vesicles which were not found in the intervaricosities. The neuromuscular gaps, the distances between the axon terminals and smooth muscle cells, were usually interposed with connective tissues, fibroblasts or Schwann cell processes. The neuromuscular distance for NPY-positive varicosities was $731 \pm 5$ nm (26 varicosities) in the mesenteric artery and $1304 \pm 166$ nm (12 varicosities) in the renal artery; there were no notable differences between the experimental groups.

*Immunolabelling of perivascular nerves*

Perivascular nerve fibres (axons) immunoreactive for the antigens examined were present mainly in nerve bundles, but also in a few solitary axon profiles enclosed by basal lamina or processes of Schwann cells (Figs 1–3). In general, the density of TH and NPY-immunopositive nerve bundles did not appear to vary between the groups of animals examined (qualitative observation). Immunopositive and negative axons were seen either associated with, or free from, Schwann cell processes. The labelled axons showed electron-dense immunoreactive particles in the axoplasm and/or the membranes of mitochondria in varicosities and microtubules mainly in intervaricose regions. The intensity of labelling of different nerve profiles was variable, but in all cases positive nerve fibres could clearly be distinguished from neighbouring negative ones.

In general, TH, NPY, NOS and VIP-immunopositive axons were observed in the mesenteric arteries of each animal group examined, but no SP-immunolabelled axons were seen. In the renal artery, TH and NPY-immunoreactive axons were demonstrated in all 4 groups, but immunoreactive axon profiles for VIP were observed only sparsely and only in the cold control group; neither SP nor NOS-immunostained axon profiles were observed in any animal group. The percentage of axon profiles positive for TH, NPY, NOS, VIP, and SP are shown in the Table and examples of the distributions of immunostained perivascular nerves are displayed in Figs 1–3.

*Immunolabelling for TH*

TH-immunoreactive axon profiles of normothermic control, cold control, hibernated and aroused hamster mesenteric and renal arteries (Fig. 1) exhibited mostly vesicles and mitochondria (Fig. 1*c*). A large number of axons positive for TH were observed in mesenteric and renal arteries of hibernating animals (Fig. 1*d*, *e*). Following 2 h arousal from hibernation, most nerve bundles had a comparable appearance to the controls (cf. Fig. 1*f* with 1*a*).

*Immunolabelling for NPY*

NPY-immunoreactive axon profiles (Fig. 2*a–i*) showed mitochondria and small and large vesicles (Fig. 2*b*); the central core of some large granular vesicles was immunolabelled (Fig. 2*b*, *f*). The mesenteric and renal arteries of hibernating animals displayed the highest number of axon profiles labelled for NPY (Fig. 2*e–g*).

*Immunolabelling for NOS*

Axons positively-labelled for NOS-I were sparse in the mesenteric arteries from all groups of animals examined (Fig. 3*a–e*). No NOS-I-immunoreactive axons were observed in the renal arteries.

*Immunolabelling for VIP*

Axon profiles immunolabelling for VIP (Fig. 3*f–h*) displayed mitochondria and small agranular and large granular vesicles (Fig. 3*f*,*h*); the central core of some granular vesicles contained immunoprecipitate. Fewer VIP-positive axon profiles were observed in hibernating mesenteric arteries compared with normothermic controls. Renal artery exhibited no VIP-immunolabelled nerve fibre profiles, apart from an occasional axon profile in the cold-exposed control group.

*Immunolabelling for SP*

No SP-immunolabelled axon profiles were observed in either mesenteric or renal arteries.

*Percentages of TH, NPY, NOS, VIP, SP-immunopositive axon profiles*

Data representing the percentages of TH, NPY, NOS, VIP and SP-immunoreactive axon profiles of mesenteric and renal arteries of normothermic control, cold control, hibernating and aroused hamsters are given in the Table. There was a striking increase in the percentage of immunoreactive axons for TH and

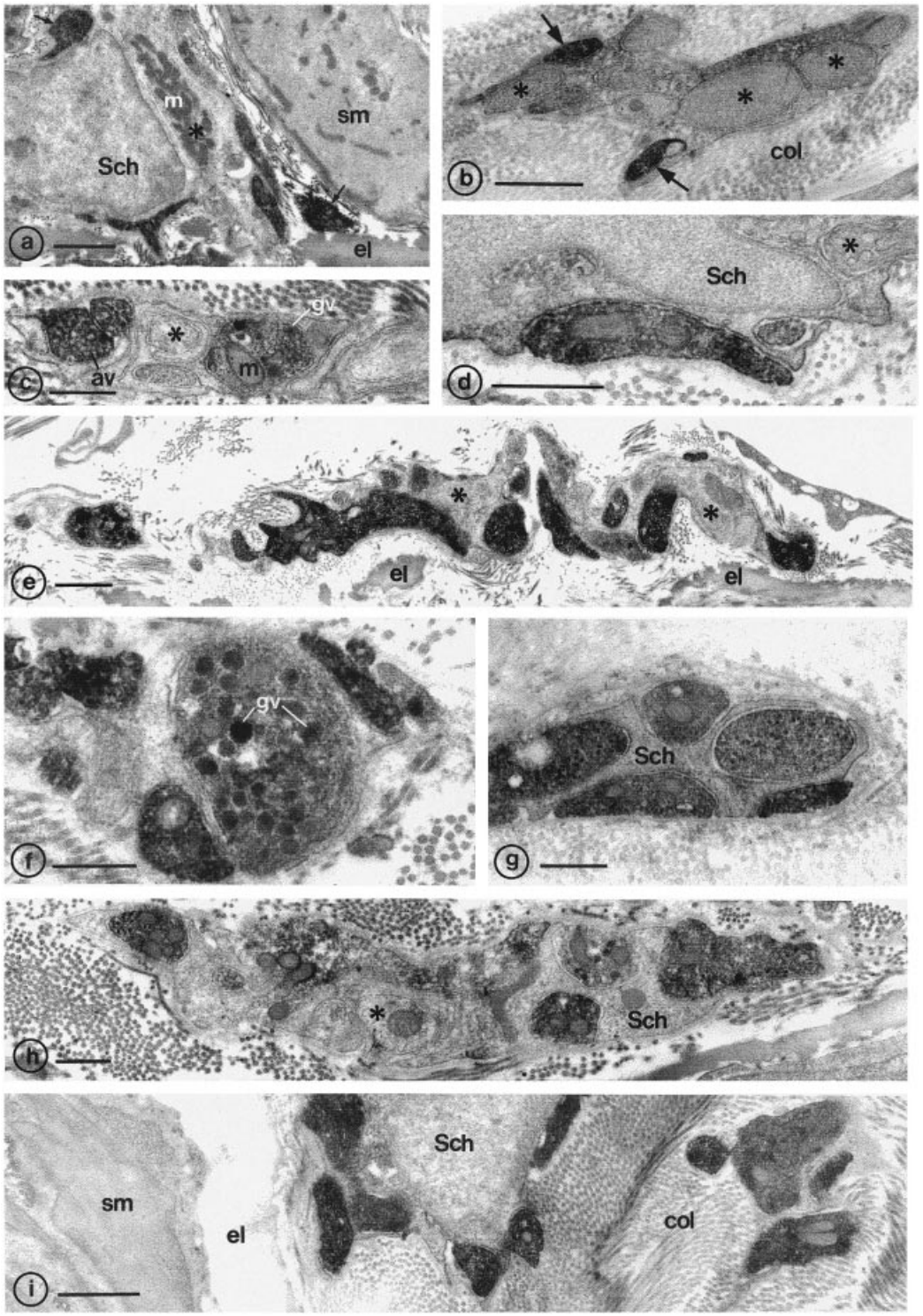


Fig. 2. Mesenteric artery (*a*, *c*, *e*, *f*, *h*) and renal artery (*b*, *d*, *g*, *i*) labelled for NPY in normothermic control (*a*, *b*), cold control (*c*, *d*), hibernating (*e*, *f*, *g*) and aroused (*h*, *i*) hamsters. (*a*) A nerve bundle showing NPY-positive axon profiles (arrows); NPY-negative axon profile (asterisk) containing numerous mitochondria (m) and unlabelled Schwann cell (Sch) can also be seen. sm, Smooth muscle; el, external elastic lamina. (*b*) Two NPY-positive and many NPY- negative axon profiles are seen in a nerve bundle. col, Collagen fibres. (*c*) Higher magnification of NPY-positive varicosities showing agranular (av) and granular (gv) vesicles and mitochondria. Unlabelled axon profiles are also seen. (*d*) Nerve bundle showing NPY-positive and NPY-negative axon profiles associated with a Schwann cell. (*e*) Several NPY-positive axon profiles lie along the side of adventitial medial border. NPY-negative axon profiles can also be seen. (*f*) A higher magnified portion of nerve bundle contain many NPY-positive axon profiles. Note large granular vesicles (gv) displaying labelled cores in a varicosity. (*g*) A nerve bundle showing several NPY-positive axon profiles are incompletely enclosed in Schwann cell processes. (*h*) A nerve bundle showing NPY-positive and NPY-negative axon profiles. (*i*) A nerve bundle showing many NPY-positive axon profiles associated with a Schwann cell. Bars, *a*, *e*, *i*, 1 μm; *b*, *c*, *d*, *f*, *g*, *h*, 500 nm.

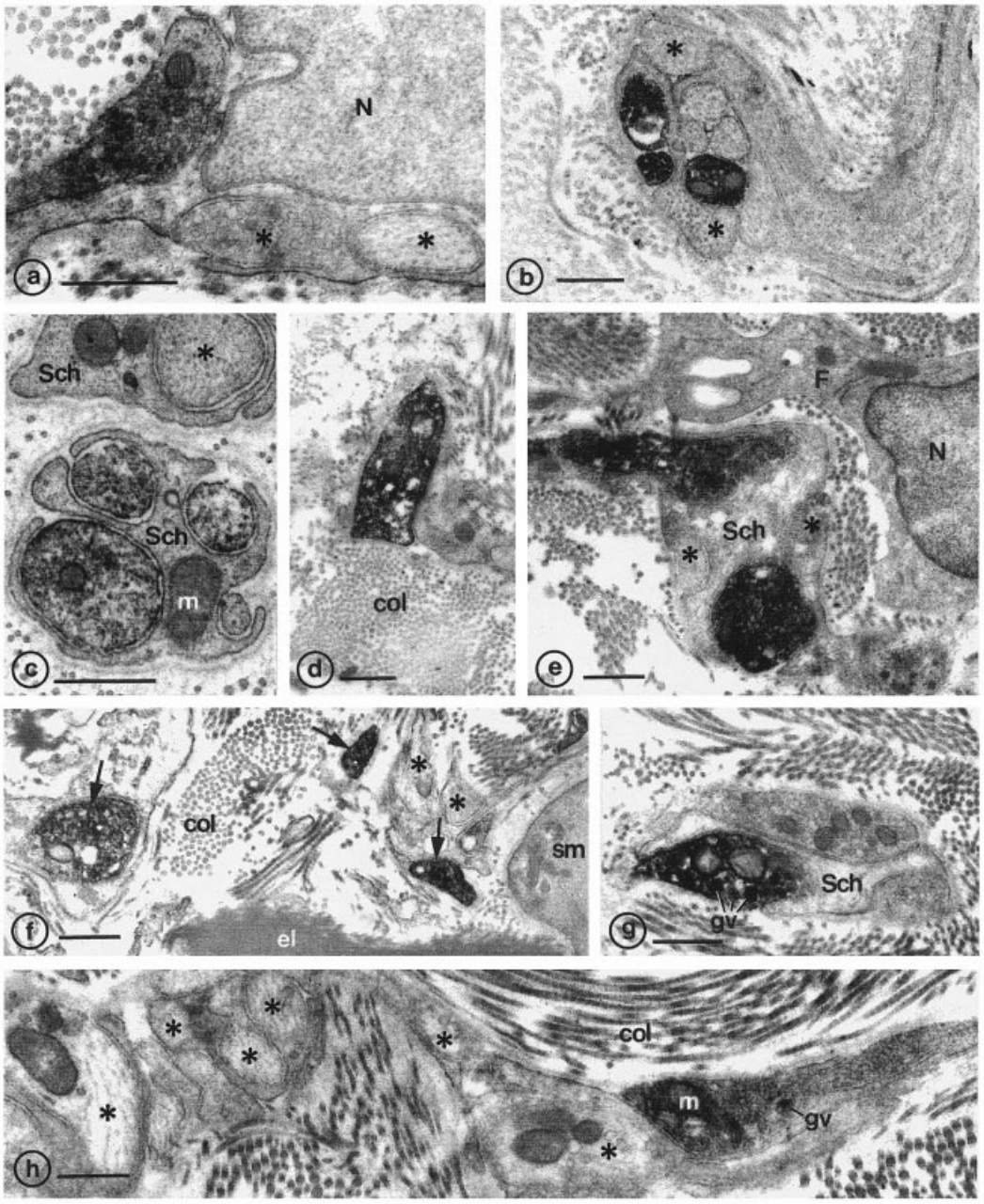


Fig. 3. Mesenteric artery. Examples of axon profiles labelled for NOS (*a–e*), and VIP (*f–h*) in normothermic control (*a*, *f*), cold control (*b*, *g*), hibernating (*c*, *d*, *h*) and aroused (*e*) hamsters. (*a*) NOS-positive axon profile showing moderate immunoreaction. Unlabelled axon profiles (asterisks) are seen. N, Schwann cell nucleus. (b) Portion of nerve bundle showing 3 heavily NOS-labelled axons among NOS-negative ones. (*c*) Higher magnification of nerve bundles showing NOS-positive and NOS-negative axon profiles incompletely enclosed in Schwann cell processes (Sch). m, Mitochondrion; col, collagen fibres. (*d*) NOS-positive axon profiles showing strong immunoreaction. (*e*) Nerve bundle showing 2 prominent NOS-positive and 2 negative axon profiles. F, fibroblast; N, nucleus. (*f*) Electron micrograph showing VIP-positive (arrows) and VIP-negative (asterisks) axon profiles. sm, smooth muscle; el, external elastic lamina. (*g*) Higher magnification of portion of nerve bundle showing VIP-positive and VIP-negative varicosities. Note VIP-positive varicosity displaying heavy immunoreaction in large granular vesicles (gv). (*h*) Nerve bundle containing 1 VIP-positive and several VIP-negative axon profiles. Note VIP-positive varicosity showing the immunoprecipitation in large granular vesicle and attached to membrane of mitochondria. Bars, *a–h*, 500 nm.

NPY in both mesenteric and renal arteries from hibernating hamsters as compared with the remaining 3 groups. After 2 h arousal from hibernation, the percentage of TH and NPY-immunopositive axons was reduced compared with the hibernating group, but was still higher than those of the 2 control groups. The percentage of axons immunolabelling for NOS in the mesenteric arteries was slightly increased in hibernation compared with the other groups. For VIP, the percentage of positive axon profiles in the mesenteric artery was reduced in the cold controls and in the hibernating group.

Table. *Percentages of mesenteric and renal artery axon profiles of normothermic control, cold control, hibernating and aroused hamsters showing immunoreactivity to TH, NPY, NOS, VIP and SP*

| | Percentages of immunopositive axon profiles | | | | |
|---|---|---|---|---|---|
| | TH | NPY | NOS | VIP | SP |
| *Mesenteric artery* | | | | | |
| Normothermic control (n = 3) | 17.0 ± 0.9 (1164) | 29.9 ± 3.0 (1244) | 1.2 ± 0.3 (1557) | 14.3 ± 1.2(1530) | 0 (967) |
| Cold control (n = 3) | 22.1 ± 2.1 (1956) | 27.6 ± 2.7 (1718) | 1.7 ± 0.4 (1778) | 6.4 ± 1.0 (1806) | 0 (831) |
| Hibernating (n = 2) | 57.0 ± 1.3 (1126)* | 65.2 ± 1.8 (1607)* | 7.5 ± 0.7 (1033)* | 3.8 ± 0.4 (1540)$^{+}$(n = 3) | 0 (795) |
| Aroused (n = 2) | 33.2 ± 2.1 (1167) | 44.2 ± 3.9 (1141) | 2.8 ± 0.9 (1151) | – | – |
| *Renal artery* | | | | | |
| Normothermic control (n = 3) | 19.6 ± 2.3 (1573) | 25.5 ± 2.0 (1527) | 0 (1387) | 0 (1529) | 0 (1381) |
| Cold control (n = 3) | 22.3 ± 2.7 (1400) | 35.0 ± 1.9 (1638) | 0 (1448) | 0.1 ± 0.2 (1396) | 0 (916) |
| Hibernating (n = 2) | 75.8 ± 1.3 (1306)* | 76.8 ± 1.7 (1297)* | 0 (927) | 0 (1020) | 0 (850) |
| Aroused (n = 2) | 53.0 ± 6.7 (1394) | 49.2 ± 3.4 (1596) | 0 (968) | – | – |

Data expressed as mean ± S.E.M. from at least 12 sections per animal group. Number of axon profiles examined in parenthesis. n = number of animals used. *$P < 0.05$ compared to controls and aroused animals. $^{+}P < 0.05$ compared to normothermic controls.

## DISCUSSION

The current study shows a remarkable increase in the immunoreactivity for the sympathetic nerve markers TH and NPY in perivascular nerves in both mesenteric and renal arteries of hibernating hamsters. Two hours after arousal from hibernation, the percentage of TH and NPY-immunoreactive nerve profiles was reduced, but it was still higher than those of normothermic and cold control animals. This increase is consistent with reports of high peripheral vascular resistance and of increased sympathetic nerve activity during hibernation (Lyman, 1965; Nedergaard & Cannon, 1990). A decrease in immunoreactivity of the sympathetic markers 2 h after arousal from hibernation indicates a rapid mechanism for return of sympathetic nerve activity to normality.

Previous immunohistochemical studies for NA and NPY at the light microscope level did not reveal any obvious changes in the density of the sympathetic nerve supply in the mesenteric artery during hibernation (Ralevic et al. 1997). This may reflect our findings of no apparent change in the density of TH and NPY-immunopositive nerve bundles in hibernation. However, at the electron microscope level, an increase in number of immunopositive axons per nerve bundle were noted; these changes would not necessarily be detectable at the light microscope level. The percentage of NPY-positive axon profiles was often slightly higher than the percentage of TH-positive axon profiles. This may be due to actual differences in expression or to differences in avidity of the respective antibodies used for the immunodetection. Our present data give no information of possible hibernation-induced changes in TH activity, as opposed to TH content, or of levels of NA in the varicosities.

In addition to increased sympathetic nerve activity, there is evidence for enhancement of postjunctional responses to NA in vessels of hibernating woodchuck and hedgehog (Eliassen & Helle, 1975; Miller et al. 1986) and in pre- and postjunctional modulatory responses in hamster mesenteric arteries (Ralevic et al. 1997, 1998). In most blood vessels, NPY, costored and coreleased with NA from sympathetic nerves, acts predominantly as a postjunctional neuromodulator, producing a powerful potentiation of noradrenergic vasoconstriction (Ekblad et al. 1984; Pernow et al. 1986). Lack of functional responses to NPY in hamster mesenteric arteries suggests a neuromodulatory role in this vessel (Hill et al. 1996). The distance between the NPY-containing varicosities and adjacent smooth muscle in hamster mesenteric and renal arteries is consistent with a predominantly postjunctional neuromodulatory action for NPY (Burnstock, 1990; Owen, 1993).

Potent vasodilator responses to exogenous VIP have been reported in the hamster mesenteric arterial bed (Hill et al. 1996). In the present study, a relatively high percentage of VIP-immunoreactive axon profiles were observed in the mesenteric artery of normothermic hamsters, but fewer were evident in the cold controls with even less in the hibernating animals. A decrease in immunoreactivity for this parasympathetic vasodilatory neuropeptide during hibernation may contribute to the observed increased vascular resistance at least in the mesenteric bed. In contrast, there were virtually no VIP-immunoreactive nerves in the renal arteries of any of the hamsters examined

suggesting that VIP does not play a role in renal vascular control in this species.

There was a sparse innervation of the hamster mesenteric artery by NOS-positive nerves. The percentage of NOS-containing axon profiles increased during hibernation, returning towards the control levels during arousal. It is not clear which population of nerves are the source of this increase in NOS. NOS-positive nerve profiles were absent from the hamster renal artery. As VIP and CGRP-immunoreactive axon profiles were also only detected in the mesenteric artery (see later) it is likely that in these animals, NOS is localised in parasympathetic and/or sensory-motor nerves. The lack of vasodilator transmitters in hamster renal artery perivascular nerves, as demonstrated in the present study, highlights the importance of NO released from the endothelium in the control of vascular tone in this vessel. Our previous studies have shown that the percentages of both NOS-positive and endothelin-positive endothelial cells of the mesenteric and renal arteries are notably lower in hibernating hamsters than in control animals and following arousal from hibernation (Saitongdee et al. 1999). These changes may reflect a reduced endothelial contribution to the maintenance of vascular tone during hibernation. The present findings indicate that this occurs in concert with a marked increase in sympathetic innervation, supporting a predominantly vasoconstrictor control of mesenteric and renal arteries during hibernation.

There were no perivascular nerves immunoreactive for SP in either mesenteric or renal arteries from any of the animal groups examined. A sparse supply of calcitonin gene-related peptide-containing nerves was detected in the mesenteric artery, but there were none in the renal artery (unpublished observation). The presence of calcitonin gene-related peptide, but not SP, in the hamster mesenteric artery concurs with a previous report (Hill et al. 1996). Sensory-motor nerves may not participate in regulating blood flow in hamster mesenteric artery, whereas they have an efferent vasodilatory function via calcitonin gene-related peptide release in rat mesenteric arteries (Kawasaki et al. 1988; Hill et al. 1996).

The rapid decrease in percentage of TH, NPY, and NOS-immunoreactive axons only 2 h after arousal raises interesting questions about the mechanisms involved. As it is unlikely that retraction of nerves would occur during this time scale, the observations could be due to decreased expression of the sympathetic markers and/or their depletion from the varicosities. It should be noted that axon profiles counted included both varicosities and intervaricosities. A reduction in the mRNA expression of the markers at the level of the sympathetic ganglia and consequent reduction in axonal transport of the end product to the terminal varicosities may bring the levels in the intervaricosities to below that of immunodetection. Changes in gene expression of TH and NPY can occur rapidly, within hours, for example in the superior cervical ganglion after axotomy (Zigmond et al. 1998) and in the adrenal gland after cold exposure (Baruchin et al. 1990). Identification of genes differentially expressed in ganglia during the regulated processes of entrance into and arousal from hibernation when there are marked changes in autonomic control will shed light on the molecular mechanisms involved and are currently underway in our laboratory.

To summarise, the increase in immunoreactivity for the markers TH and NPY for sympathetic nerves mediating vasoconstriction and concomitant decrease in immunoreactivity of VIP the marker for parasympathetic nerves mediating vasodilatation, are consistent with evidence for an increase in peripheral vascular resistance in hibernating animals.

## ACKNOWLEDGEMENTS

This work was supported by the British Heart Foundation.

## REFERENCES

BARUCHIN A, WEISBERG EP, MINER LL, ENNIS D, NISENBAUM LK, NAYLOR E et al. (1990) Effects of cold exposure on rat adrenal tyrosine hydroxylase: an analysis of RNA, protein, enzyme activity, and cofactor levels. *Journal of Neurochemistry* **54**, 1769–1775.

BURNSTOCK G (1990) Co-transmission. The Fifth Heymans Lecture, Ghent. *Archives Internationales de Pharmacodynamie et de Therapie* **304**, 7–33.

BURNSTOCK G, RALEVIC V (1994) New insights into the local regulation of blood flow by perivascular nerves and endothelium. *British Journal of Plastic Surgery* **47**, 527–543.

CHATFIELD PO, LYMAN CP (1950) Circulatory changes during the process of arousal in the hibernating hamster. *American Journal of Physiology* **163**, 566–574.

EKBLAD E, EDVINSSON L, WHALESTEDT C, UDDMAN R, HAKANSON R, SUNDLER F (1984) Neuropeptide Y co-exists and co-operates with noradrenaline in perivascular nerve fibers. *Regulatory Peptides* **8**, 225–235.

ELIASSEN E, HELLE KB (1975) Spontaneous activity in smooth muscle of the portal vein of the hedgehog *Erinaceus europaeus L. Comparative Biochemistry and Physiology C* **52**,119–125.

HILL B, RALEVIC V, CROWE R, BURNSTOCK G (1996) Innervation and nitric oxide modulation of mesenteric arteries of the golden hamster. *European Journal of Pharmacology* **317**, 275–283.

HISA Y, UNO T, TADAKI N, UMEHARA K, OKAMURA H, IBATA Y (1995) NADPH-diaphorase and nitric oxide synthase in the canine superior cervical ganglion. *Cell and Tissue Research* **279**, 629–631.

HOLZER P, WACHTER C, HEINEMANN A, JOCIC M, LIPPE IT, HERBERT MK (1995) Sensory nerves, nitric oxide and NANC vasodilatation. *Archives Internationales de Pharmacodynamie et de Therapie* **329**, 67–79.

KAROON P, KNIGHT G, BURNSTOCK G (1998) Enhanced vasoconstrictor responses in renal and femoral arteries of the golden hamster during hibernation. *Journal of Physiology* **512**, 927–938.

KAWASAKI H, TAKASAKI K, SAITO A, GOTO K (1988) Calcitonin gene-related peptide acts as a novel vasodilator neurotransmitter in mesenteric resistance vessels of rat. *Nature* **335**, 164–167.

LYMAN CP (1965) Circulation in mammalian hibernation. In: *Handbook of Physiology*, Section 2, *Circulation*, Vol. 3, pp. 1967–1990. Washington, DC: American Physiological Society.

LYMAN CP, O'BRIEN RC (1988) A pharmacological study of hibernation in rodents. *General Pharmacology* **19**, 565–571.

MAGGI CA. MELI A (1988) The sensory-efferent function of capsaicin-sensitive sensory nerves. *General Pharmacology* **19**, 1–43.

MILLER VM, MILLER WL, SOUTH FE (1986) Vascular smooth muscle responsiveness in a hibernator: effects of season and temperature. *American Journal of Physiology* **250**, R77–R82.

NEDERGAARD J, CANNON B (1990) Mammalian hibernation. *Philosophical Transactions of the Royal Society of London*, *Series B*, *Biological Sciences* **326**, 669–686.

NOZAKI K, MOSKOWITZ MA, MAYNARD KI, KOKETSU N, DAWSON TM, BREDT DS et al. (1993) Possible origins and distribution of immunoreactive nitric oxide synthase-containing nerve fibres in cerebral arteries. *Journal of Cerebral Blood Flow and Metabolism* **13**, 70–79.

NÜRNBERGER F (1995) The neuroendocrine system in hibernating mammals: present knowledge and open questions. *Cell and Tissue Research* **281**, 391–412.

OKAMURA T, YOSHIDA K, TODA N (1995) Nitroxidergic innervation in dog and monkey renal arteries. *Hypertension* **25**, 1090–1095.

OWEN MP (1993). Similarities and differences in the post-junctional role for neuropeptide Y in sympathetic vasomotor control of large vs. small arteries of rabbit renal and ear vasculature. *Journal of Pharmacology and Experimental Therapeutics* **265**, 887–895.

PERNOW J, SARIA A, LUNDBERG JM (1986) Mechanism underlying pre- and post-junctional effects of neuropeptide Y in sympathetic vascular control. *Acta Physiologica Scandinavica* **126**, 239–249.

RALEVIC V, HILL B, CROWE R, KNIGHT G, BURNSTOCK G (1997). Effects of hibernation on neural and endothelial control of mesenteric arteries of the golden hamster. *American Journal of Physiology* **273**, H148-H155.

RALEVIC V, KNIGHT G, BURNSTOCK G (1998) Effects of hibernation and arousal from hibernation on mesenteric arterial responses of the golden hamster. *Journal of Pharmacology and Experimental Therapeutics* **287**, 521–526.

SAITONGDEE P, LOESCH A, KNIGHT G, MILNER P, BURNSTOCK G (1999) Ultrastructural localization of nitric oxide synthase and endothelin in the renal and mesenteric arteries of the golden hamster: differences during and after arousal from hibernation. *Endothelium* **6**, 197–207.

SHENG H, GAGNE GD, MATSUMOTO T, MILLER MF, FORSTERMANN U, MURAD F (1993) Nitric oxide synthase in bovine superior cervical ganglion. *Journal of Neurochemistry* **61**, 1120–1126.

VIALS AJ, CROWE R, BURNSTOCK G (1997) A neuromodulatory role for neuronal nitric oxide in the rabbit renal artery. *British Journal of Pharmacology* **121**, 213–220.

YOSHIDA K, OKAMURA T, KIMURA H, BREDT DS, SNYDER SH, TODA N (1993) Nitric oxide synthase-immunoreactive nerve fibers in dog cerebral and peripheral arteries. *Brain Research* **629**, 67–72.

ZIGMOND R, MOHNEY R, SCHREIBER R, SHADIACK A, SUN Y, VACCARIELLO YS et al. (1998) Changes in gene expression in adult sympathetic neurons after axonal injury. *Advances in Pharmacology* **42**, 899–903.